CrystEngComm

Accepted Manuscript

ROYAL SOCIETY OF CHEMISTRY

www.rsc.org/crystengcomm

Dynamic Article Links ►

Cite this: DOI: 10.1039/c0xx00000x

www.rsc.org/xxxxxx

ARTICLE TYPE

The effect of nitridation temperature on the structural, optical and electrical properties of GaN nanoparticles

M. Gopalakrishnan[a], **V. Purushothaman**[a], **V. Ramakrishnan**[b], **G. M. Bhalerao**[c], **and K. Jeganathan**[a]*

Received (in XXX, XXX) Xth XXXXXXXXX 20XX, Accepted Xth XXXXXXXXX 20XX

DOI: 10.1039/b000000x

Synthesis of GaN nanoparticles by novel chemical co-precipitation method and the effect of nitridation temperature on the structural, optical and electrical properties have been reported. X-ray diffraction and high resolution transmission electron microscopy exhibit hexagonal wurtzite structure with high crystalline nature of GaN NPs. A strong blue luminescence was observed for all the GaN NPs at room temperature photoluminescence studies. Nevertheless, the red and yellow luminescence were absent for the nitridation temperature of 1000°C. The phonon frequency mode at K point of the Brillouin zone symmetry was observed at 271-273 cm^{-1} for GaN NPs by micro-Raman spectroscopy which is normally absent for bulk GaN. The carrier concentration and mobility of GaN NPs synthesized at higher temperature were calculated to be 1.36 X 10^{17} cm^{-3} and 433 cm^2/V s respectively by the Raman line shape analysis of the longitudinal-optical-phonon-plasmon coupled mode.

Introduction

Over the past few years, considerable efforts have been devoted to the research field of semiconducting nanomaterials due to their unique electronic, optical and mechanical properties which cannot be realized in their bulk counterparts that enables potential applications in sensors and optoelectronics.[1, 2] III-Nitrides (InN, GaN and AlN) are one of the important classes of semiconductor because of their direct band gap and their alloys may span a wide region in the electromagnetic spectrum from deep ultraviolet (UV) to infra-red (IR), which makes attractive for light emitting diodes (LEDs) and laser diodes (LDs).[3,4] Among the group III-Nitrides, GaN has attracted a considerable attention as a building block for the assembly of nanodevices such as UV lasers, LEDs, blue emitters and detectors [4-6] due to its wide and direct bang gap of 3.4eV and high excitonic binding energy of 20 meV. In addition, it can also be used for high power/high temperature electronic devices such as high-electron-mobility transistor and high-speed field effect transistors due to their high carrier mobility, electrical breakdown field, melting point, chemical and thermal stability.[6-9] The epitaxial GaN grown on sapphire, silicon or SiC substrates have been used to fabricate the GaN based devices in current planar technology. A major problem that hinders the fabrication of high quality GaN is due to the lack of lattice-matched nonpolar native substrates. Thus, it is more essential to synthesis bulk GaN single crystal as a suitable substrate for device applications with improved luminescence performance and life time. GaN NPs are required as a precursor material for the fabrication of GaN single crystal by sublimation,[10] high pressure solution method[11] and ammonothermal method[12] and also deposition targets for thin films. Generally, GaN NPs prepared by the reaction of Ga_2O_3 with NH_3 has high concentration of residual oxygen which increases the density of dislocation and reduces the continuous growth of GaN single crystal.[12] Hence, the scalable and novel techniques are needed for the synthesis. GaN NPs have been fabricated by various methods such as direct reaction of Ga with NH_3,[13] thermal decomposition,[14] combustion method,[15] reaction of Ga_2O_3 with NH_3,[16] ammonolysis of Ga with NH_3 using NH_4I as a catalyst[12] and soluble salt-assisted synthesis.[17] However few reports have been seen in literature for the synthesis of GaN NPs by chemical co-precipitation method, in which the properties of NPs have not been analyzed instead the synthesized NPs was used as a source material for the growth of GaN nanowires.[18] The chemical co-precipitation method offer several advantages of the large scale production, high chemical purity, low chemical processing temperature and possibility of obtaining fine particles with narrow size distributions along with the high yield over the other chemical methods. We have demonstrated the characterization of GaN NPs by chemical co-precipitation method in our previous report.[19] It was essential to specify that there are few reports on the effect of ammoniating temperature on structural, morphological and optical properties of one dimensional GaN nanostructures,[20-22] and no complete analysis on GaN NPs to our knowledge. In present work we report the role of nitridation temperature on the structural, optical and electrical properties of GaN NPs by chemical co-precipitation method.

Experimental

The experimental procedure for the synthesis of GaN NPs by chemical co-precipitation method was followed in a similar way as described in our previous report.[19] In a typical experiment, pure metal Ga (99.999%) was dissolved in HNO_3 (70%) solution with molar ratio of 1:16 under ultra-sonication for 1h. The resultant solution was diluted with 2-propanol with molar ratio of 1:90 and allowed to stirring process for 30 minutes. A slow addition of 25% NH_4OH to the solution under constant stirring results in white precipitate which was separated by centrifugation, washed in ethanol and dried at 70°C for 24 h. The products are equally divided into three parts. Nitridation process was carried out independently for all the three samples by hot wall quartz tube reactor under ammonia (NH_3) flow rate of 1000 SCCM (Standard Cubic Centimetre per Minute) for 2 h at different temperature of 900, 950 and 1000°C. The precipitated products dried at 70°C for 24 h before the nitridation and the final yellow coloured GaN powders after the nitridation process are subjected to various characterizations. The structure and phase products of the material before and after the nitridation treatment were identified by powder X-ray diffraction (XRD - Rigaku Rint 2200V) using Cu K_α radiation (λ = 1.5406 Å). The presence of functional groups in the precipitated products were examined by Fourier transform infrared spectroscopy (FTIR-JASCO 460Plus FT/IR Spectrometer) in the wave number region between 4000-400 cm^{-1}.The morphology and chemical composition of the particles were investigated by field emission scanning electron microscopy (FESEM- Carl Zeiss) equipped with energy dispersive X-ray spectroscopy (EDX- Oxford instruments). The crystalline nature of GaN NPs was analyzed by high resolution transmission electron microscopy (HRTEM – LIBRA 200 TEM - Carl Zeiss) equipped with selected area electron diffraction (SAED). TEM samples were prepared by dispersing the GaN NPs in 2-propanol by ultrasonically and casting a drop of the suspension on the carbon-coated Cu-grid. The room temperature photoluminescence (PL) was carried out by using He-Cd laser with 325 nm wavelength as a excitation source and a charge coupled device (CCD) was used to detect the luminescence signal. The optical and vibrational modes of the GaN NPs were characterized by micro-Raman scattering measurements using Ar ion laser with an excited wavelength of 488 nm with a spot size of ~ 1.0 µm and the scattered signals were collected through CCD. The electrical parameters were measured by Hall measurement set-up (ECOPIA-HMS 3000) with a permanent magnet of 0.57T at room temperature.

Results and Discussion

The XRD pattern of co-precipitated products dried at 70°C for 24h before the nitridation process is shown in Fig.1 (a). The diffraction peaks are indexed to the orthorhombic phase of gallium oxide hydroxide (GaO(OH)) (JCPDS No.:73-1028 and 26-0674). A sharp (220) peak indicates good crystalline quality of the precipitated products. No other crystalline or mixed phases of Ga_2O_3 and $Ga(OH)_3$ present in the XRD pattern which evidences the pure crystalline phase of GaO(OH) nanoparticles. Further, the functional groups such as Ga-O stretching modes and Ga-OH bending modes [23-25] in the FTIR spectrum as shown in Fig.S1 also confirms the pure phase of GaO(OH) material.

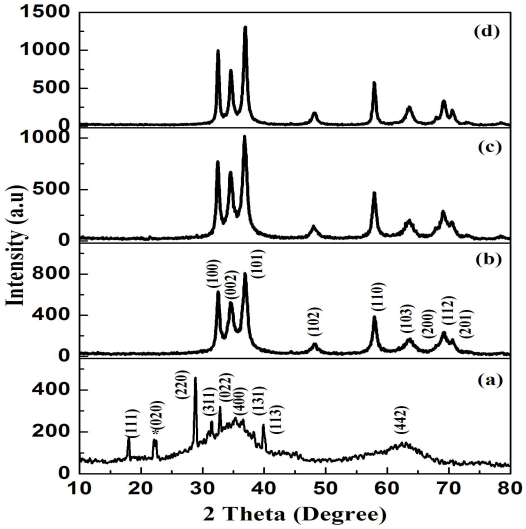

Fig.1. XRD patterns of (a) GaO(OH) and GaN NPs synthesized at (b) 900°C (c) 950°C and (d) 1000°C.

Nitridation Temperature (°C)	FWHM of (101) plane (arc-sec)	Lattice Constants (Å)		Average Particle Size (nm)
		a	c	
900	2603	3.1766	5.2100	12.85
950	2556	3.1824	5.2260	13.43
1000	1984	3.1785	5.1495	14.80

Table 1. Variation of FWHM of (101) plane, lattice parameters (a and c) and crystallite size of GaN NPs relative to the nitridation temperatures (900 -1000°C).

XRD pattern of GaN NPs nitrided at 900, 950 and 1000°C are shown in Fig.1 (b-d). The XRD patterns confirm the formation of single phase hexagonal wurtzite structure of GaN (JCPDS No: 89 – 8624) and no other crystalline phases of GaN such as cubic and gallium oxide (Ga_2O_3) peaks were found. It can be seen that the nitridation temperature increases from 900 to 1000°C, the intensity of diffracted peak also increases and attain maximum at 1000°C. This demonstrates that the crystallinity of the GaN NPs improved by the nitridation temperature. The FWHM of the (101) plane decreases with the nitridation temperature due to thermal induced coalescence of NPs at high temperature. Further, the average size of GaN NP increases with the increase of nitridation temperature (Table 1). The particle size of the GaN NPs are estimated by means of Debye - Scherrer formula,[26]

$$D = 0.9\,\lambda / (\beta \cos \theta) \quad \text{--------------------} \ (1)$$

where λ is the wavelength of X-ray beam used (λ= 1.5406 Å for Cu Kα radiation), θ the peak position of the given (hkl) peak and β the corresponding FWHM in radian. The variation of FWHM for (101) plane, lattice parameters (a and c), and the average crystallite size of GaN NPs relative to nitridation temperatures (900 -1000°C) are shown in Table 1.

FESEM images of GaN NPs synthesized at 900-1000°C are shown in Fig.2 (a-c) respectively. The NPs are agglomerated due to the van der Waals forces of attraction between the particles which is consistent with earlier reports.[15,19] The characteristic particle size histogram for the corresponding FESEM images are shown as insets in Fig.2(a-c). The calculated geometric mean diameter of the GaN NPs ammoniated at 900, 950 and 1000°C was found to be 29, 31 and 61nm respectively. Thus all the samples contain aggregated nanocrystallites with larger diameter

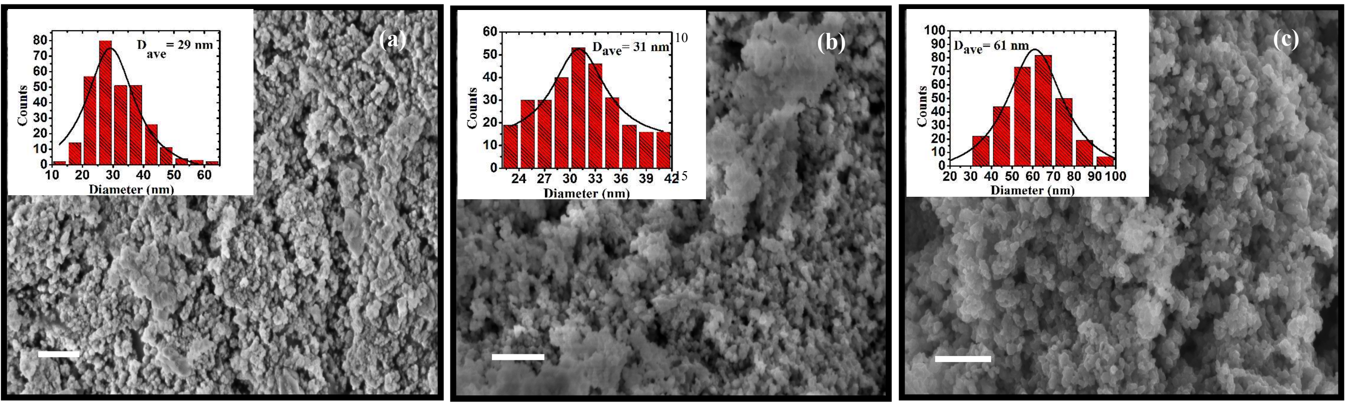

Fig.2.FESEM images of GaN NPs synthesized at (a) 900°C (b) 950°C and (c) 1000°C. Scale bar shows 200 nm. Inset figure shows the particle size histogram of corresponding FESEM images with average diameter.

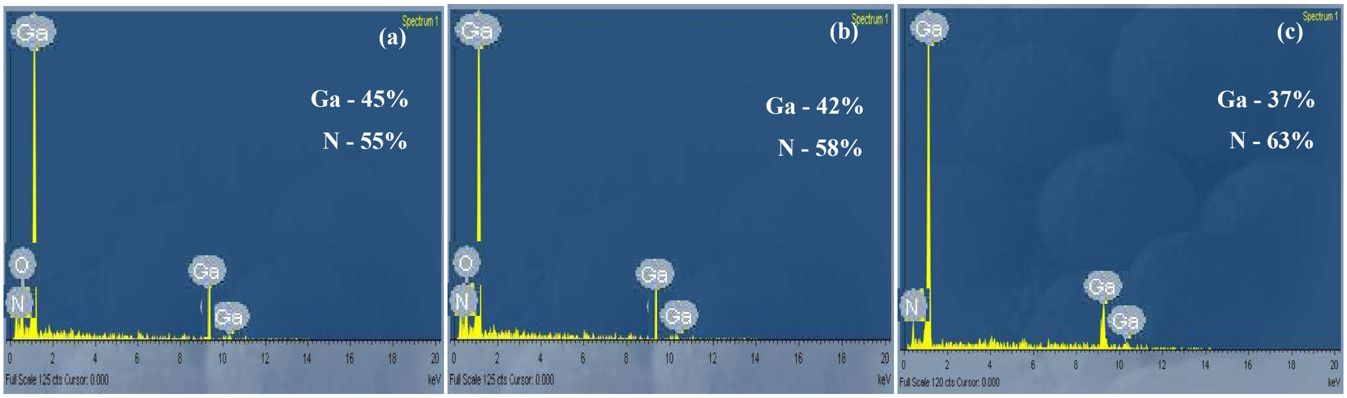

Fig.3. EDX spectra of GaN NPs synthesized at (a) 900°C (b) 950°C and (c) 1000°C.

as compared to the XRD analysis which might be due to the coalescence of NPs with respect to temperature. Since the Scherer's formula depends on the FWHM of diffracted peaks, the variation in crystallite size between XRD and FESEM were quite common. However the growth parameters such as nitridation temperature and duration are playing a major role to control the size of the NPs.

Figure 3(a-c) shows the elemental analysis carried out using EDX which confirm the N-rich GaN NPs. However the percentage of Ga was decreased when increasing the nitridation temperature owing to the evaporation of Ga at elevated temperature. Further the higher flow rate of NH_3 and its cracking efficiency may be the reason for the N-rich GaN NPs. The trace of O peak in the samples ammoniated at 900°C and 950°C are due to the unavoidable surface oxidation in NPs [17], whereas the O peak is absent for GaN NPs synthesized at 1000°C which reveals the high chemical purity. The Ga - vacancy is expected to be dominantly present for the samples annealed at 1000°C.

Transmission electron microscopy images of GaN NPs synthesized at various temperatures along with particle size distribution are shown in Fig.4 (a) and (b), which clearly indicate the spherical like particles. The average diameter of the particles is increased from 2.1 nm to 7.5 nm as the increase of the nitridation temperature from 900 to 1000°C. In general, the particle size measured from XRD is larger than the size obtained from TEM analysis since the X-ray analysis is relative to the average particle volume while the particle size calculated from TEM images correspond to the average radius. Figure 4(c) also display the HRTEM images of single GaN NP with clear lattice fringes, confirms the high crystalline nature of GaN. It should be noted that, the lattice spacing of 2.43Å corresponding to the (101) interplanar distance slightly increased to 2.47Å as the increase of the nitridation temperature from 900°C to 950°C and further the lattice spacing decreases to 2.39Å for 1000°C. Thus, the variation of d-spacing with the nitridation temperature corroborates a slight change in the lattice constants of the GaN NPs as shown in table 1. Selected area electron diffraction (SAED) pattern of NPs are shown in Fig.4 (d) which confirms the hexagonal wurtzite structure of GaN and the additional diffracted spots are emerged from the collection of NPs illustrating polycrystalline nature.

Room temperature PL spectra of GaN NPs synthesized at various temperatures are shown in Fig.5 (a-c), which depict the non-existence of near band edge (NBE) emission in all the samples. However, in our previous report a weak NBE emission was observed at 3.43eV.[19] TEM analysis shows that the particle size of GaN NPs vary from ~ 2.1 to 7.5 nm which has low magnitudes as compared to the previous report. Further, it should be noted that the band gap related emission for GaN NPs synthesized by various techniques can be observed for particles with larger size.[13-16] It was also observed that the NBE emission is enhanced for GaN NPs when the diameter of the NPs are increased to larger size.[15] Hence, a detailed investigation is need to be carried out to understand the band gap related emission with respect to particle size and will be reported in the forthcoming article.

Despite the non-existence of NBE emission, all the spectra show a very strong blue luminescence (BL) band at 2.88 eV which is often observed in GaN NPs. It is well understood that, tiny nanoparticles have large surface area with unsaturated dangling bonds, which is saturated by bonding with neighbouring

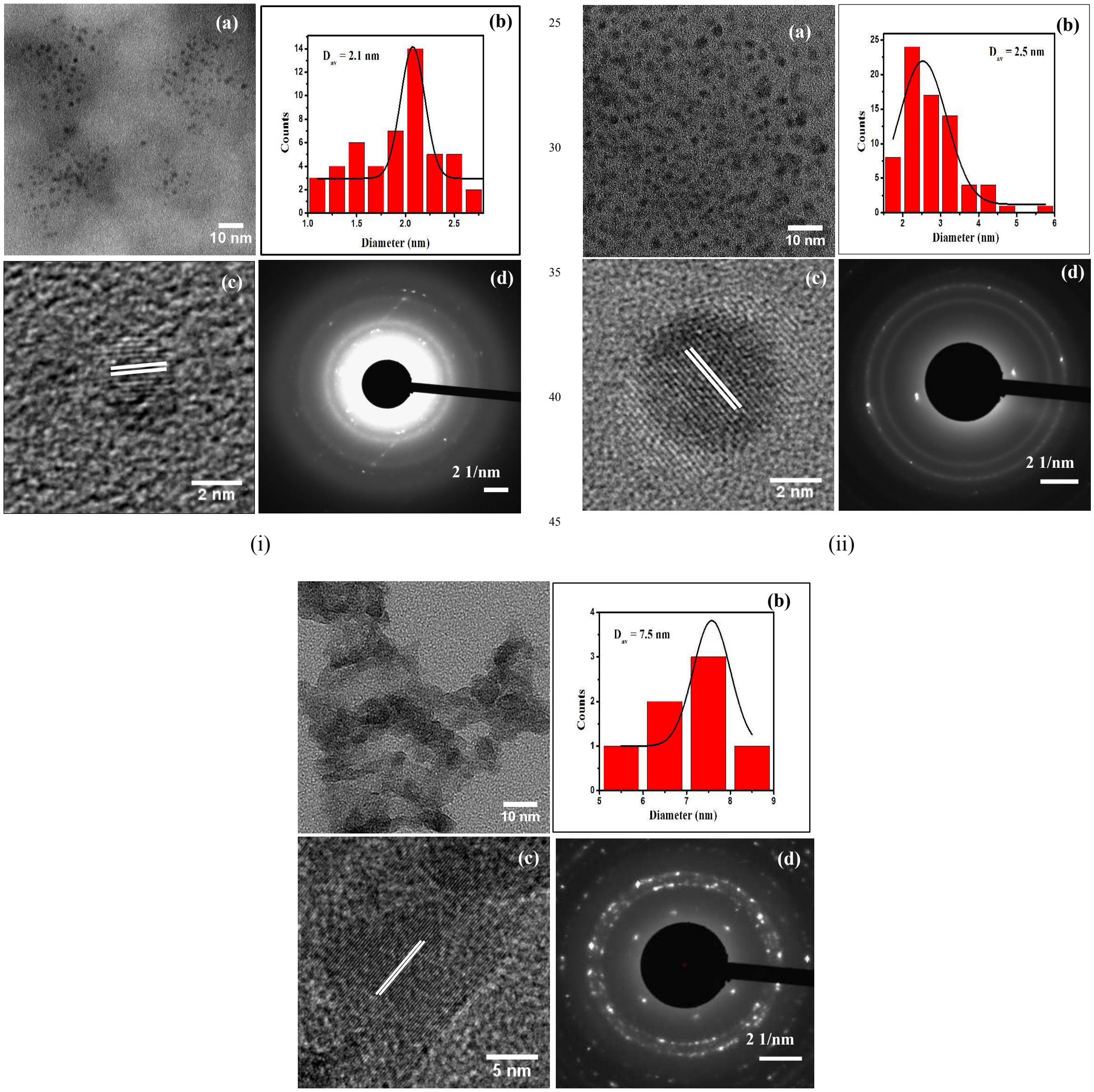

(i) (ii)

(iii)

Fig.4. TEM images of GaN NPs fabricated at various temperatures (i) 900°C (ii) 950°C and (iii) 1000°C. (a) TEM image (b) particle size Histogram (c) HRTEM image and (d) SAED pattern.

impurities. Further the exposure of GaN nanoparticles to atmosphere leads to change or formation of the surface states that affect the optical and electrical properties of GaN. The surface states in the lower part of the band gap form radiative recombination with optical excitation in the region corresponds to BL band. However the BL emission in undoped GaN was reported to be the transition from the conduction band to a relatively deep acceptor level and the defect responsible for BL emission can be attributed to the V_{Ga} - related defect complex[27] and thus consistent with EDX analysis of Ga to N ratio. In addition to the BL band, the other defect related emission such as green luminescence (GL), yellow luminescence (YL) and red luminescence (RL) were also present in the spectrum at 2.66 eV, 2.27 eV and 2.02 eV respectively for GaN NPs grown at 900ºC. The YL band is commonly observed for GaN around 2.2 - 2.25 eV. RL band can be attributed to the surface defect related emission.[27] It should be noted that the defect related emissions such as YL, BL and RL bands in GaN NPs were also often reported.[15,19] However, fascinatingly we observed that the intense YL and RL peaks are suppressed at 950ºC while GL peak intensity is increased. The YL and RL bands disappear with no change in GL band as the temperature reaches maximum of 1000ºC. It is worth to note that, GaN NPs synthesized at 1000ºC has good optical quality as compared to low temperature nitridation, which illustrates that nitridation at high temperature, is significant to enhance the optical properties of GaN NPs.

Group theory predict that, $A_1(z) + 2B_1 + E_1(x, y) + 2E_2$ optical modes at the Γ point of the Brillouin zone of hexagonal GaN [28,29] in which A_1 and E_1 modes are both Raman and infrared active, two E_2 modes are Raman active and the remaining two B_1 modes

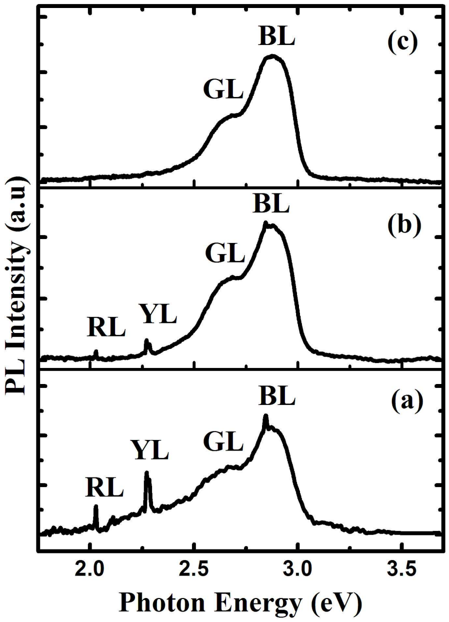

Fig.5. Room temperature PL spectra of GaN NPs synthesized at (a) 900°C (b) 950°C and (c) 1000°C.

are Raman-inactive or optically silent. The A_1 and E_1 modes are split into longitudinal optical (LO) and transverse optical (TO) components due to the polar nature. Fig.6 (a-c) shows the micro-Raman scattering spectra of GaN NPs synthesized at temperatures from 900-1000°C respectively. Raman active modes such as E_2 (low), E_2 (high), A_1 (TO), E_1 (TO) and A_1 (LO) symmetries are present in all the GaN NPs irrespective of nitridation temperature. In addition to the above Raman active bands, three additional modes are observed in all the samples which were not observed in bulk GaN. However, the strong E_2 (high) phonon mode in all the spectra reflects the characteristics of the hexagonal wurtzite structure of GaN. Further the sample prepared at 1000°C has a high intensity and sharp E_2(high) phonon peak (2.5 cm^{-1}) which exposes high crystalline quality of the GaN NPs which is consistent with the XRD results. The peak position of E_2 (high) phonon modes shift towards the higher wave number side of the spectra by1 cm^{-1} while increasing the temperature from 900 - 1000°C. The variation of FWHM of E_2 (high) and A_1 (LO) phonon modes of GaN NPs synthesized at different temperatures are shown in Fig.7 which is consistent with the XRD (Table 1). The new peaks at about 250-252 cm^{-1} and 421-423 cm^{-1} can be assigned to the zone boundary phonons (ZBP).[30] Further the Raman silent modes of ZnO [31] and GaN [29] were reported at ~276 cm^{-1} and 320-340 cm^{-1} respectively. However, Raman peak at about 271-273 cm^{-1} for GaN NPs can be attributed to the phonon frequency mode at K point of the Brillouin zone in wurtzite GaN as evidenced by adiabatic bond-charge model.[32,19]

It is worth to note that the peak position of A_1(LO) mode (738.5cm^{-1}) of GaN NPs synthesized at 1000°C shows a shift to higher frequency about 3.5cm^{-1} as compared to strain free GaN (735cm^{-1}). The shift signifies that the increase in free carrier concentration with respect to the LO phonon mode couple with the plasmon (LOPC) through electric fields. This behaviour was exploited to estimate the carrier concentration of the material by an empirical formula (valid for $n < 1 X 10^{19}$ cm^{-3}),[33]

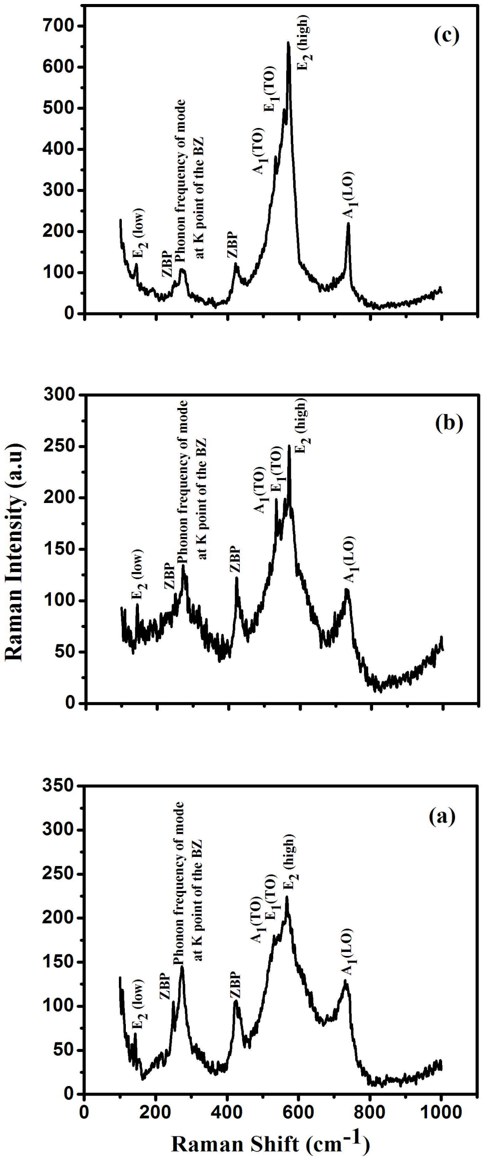

Fig.6. micro-Raman spectra of GaN NPs synthesized at (a) 900°C (b) 950°C and (c) 1000°C.

$$\mathbf{n = 1.1 X 10^{17} (\omega_{L+} - \omega_{LO})^{0.764}} \quad \text{------------ (2)}$$

where, n is the carrier concentration, ω_{L+} is the frequency of the coupled LO phonon mode and ω_{LO} is the frequency of the uncoupled LO phonon mode (ω_{LO}= 735 cm^{-1}).

However, the electrical parameters such as carrier concentration (n) and carrier mobility (μ) of the material can be precisely extracted from Raman line shape analysis of coupled LO phonon- plasmon mode. In general, electrical properties are measured by Hall-effect, capacitance – voltage (C-V) and impedance analysis. However, fabrication of electrical contacts on nanomaterials is challenging for these techniques under characterization and also they give the information about averaged transport properties of the materials over large volume of the samples. Alternatively, Raman spectroscopy has been

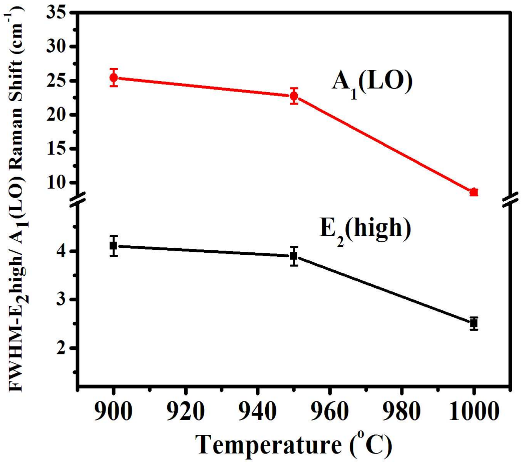

Fig.7.The variation of FWHM of E_2 (high) and A_1 (LO) phonon modes of GaN NPs synthesized at various temperatures.

widely accepted as a non-contact and effective method for low-dimensional materials system to analyze the electrical properties. Furthermore, the advantages of Raman spectroscopy over Hall and C-V measurements are non-destructive method, fast and reliable with electrical contacts enabling high spatial resolution and in-situ measurements.[34]

The carrier concentration and mobility of bulk GaN, thin films and nanowires were reported by many researchers by means of Raman line shape analysis of the LOPC mode based on the carrier scattering deformation-potential mechanism.[35-40] To the best of our knowledge, it is essential to cite that Hall and C-V measurement methods have not been applied to the extent of electrical properties of GaN NPs because of the complexity in the preparation of electrical contact to nanostructures. For that reason, in the present work, we have carried out Raman line shape analysis for GaN NPs to calculate the carrier concentration and mobility. The line shape of the coupled A_1(LO) mode of GaN NPs synthesized at 1000°C can be fitted with the values of A_1(TO) = 533cm^{-1}, A_1(LO) = 735cm^{-1}, dielectric constant ε_∞ = 5.35 and the Faust – Henry coefficient C = 0.48 as a constants followed the base line correction of the experimental data. The reproducible fitting parameters such as plasmon damping constant (γ), phonon damping (Γ) and plasmon frequency (ω_p) have been extracted from the above line shape analysis (please see supplementary information for details). The carrier concentration can be obtained from the plasmon frequency (ω_p) by using the following relation:

$$(\omega_p)^2 = \pi n e^2 / \varepsilon_\infty m^* \quad \text{------------------------ (3)}$$

where m* is the effective mass of the electron and it was determined to be 0.2m$_e$ for GaN.[38] The mobility (μ) can be estimated from the plasmon damping constant (γ) as follows:

$$\gamma = e / m^* \mu \quad \text{------------------------- (4)}$$

Figure 8 shows line shapes of the experimental (black square dots) and theoretical fitted curve (solid line) of LOPC mode for GaN NPs prepared at 1000°C. The excellent concur between the experimental and calculated line shapes of the coupled mode was observed and the carrier concentration (n) and mobility (μ) are extracted to be 1.36 X 10^{17} cm^{-3} and 433 cm^2/Vs respectively.

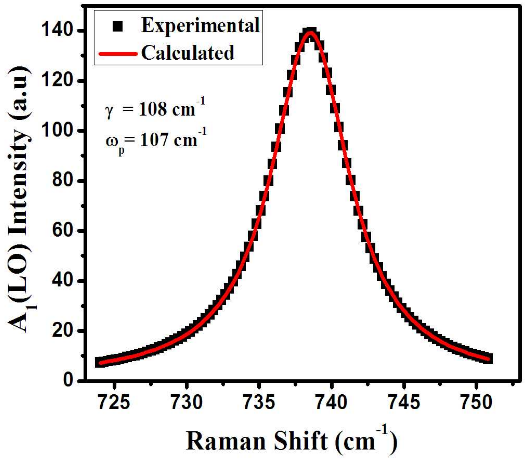

Fig.8. Experimental (black square dots) and theoretical fitted curve (solid line) of LOPC mode for GaN NPs (1000°C)

The carrier concentration obtained from Eqn. (2) is ~2.86 X 10^{17} cm^{-3}. The carrier concentration and mobility are well consistent with the reported values of GaN epitaxial layer (n = 1.5 X 10^{17} cm^{-3} for A_1(LO) = 736 cm^{-1})[37] and nanowires (n = 2.2 X 10^{17} cm^{-3}; μ = 460 cm^2 /V s for A_1(LO) = 739.4 cm^{-1})[40] by Raman line shape analysis. Hence, our results have reliable magnitude of electrical parameters. However the fitting parameters γ, Γ and ω_p obtained from line shape analysis of the LOPC mode depending on the frequency of A_1(LO) mode and act as a important role to calculate the carrier concentration and mobility of the nanomaterials.

For comparison, we have also carried out the Hall measurement to find out the electrical properties of pelleted GaN NPs. The standard van der Pauw technique was used for determination of the resistivity of uniform sample of arbitrary shape by using four small contacts placed on the periphery. In addition, the doping type, carrier concentration of the majority charge carriers and mobility of the charge carriers can also be determined by means of van der Pauw method. To facilitate the van der Pauw method, the sample thickness must be much less than the length and width of the sample and it should be symmetrical with no isolated holes. In present study, GaN pellet samples having 0.5 mm thick and 10 mm diameter were made by GaN NPs nitrided at various temperatures to characterize the electrical properties using Hall measurement system. Four indium contacts were made at the periphery of the samples in square form to ensure good Ohmic contact. The size of the contacts was made as small as possible to increase the precision of the measurements. The contacts have showed a perfect Ohmic behaviour (Fig.S2, Supplementary information) and the results are highly reproducible for various current (I).

The negative sign of Hall-co-efficient in all the samples confirm n-type conductivity of GaN NPs. The carrier concentration and mobility of GaN sample nitridated at 1000°C are 1.06 X 10^{17} cm^{-3} and 37 cm^2 / V s respectively. The mobility is considerably low as compared to Raman line shape analysis due to polycrystalline nature of GaN in which carrier scattering loss is dominant while the Raman scattering is localized non-contact method.[36] However, the carrier concentration of the GaN NPs prepared at higher temperature is comparable to that of Raman line shape analysis. Hence, Raman line shape analysis is emerged as an alternative non-contact method for the determination of carrier concentration and mobility in GaN nanoparticles.

Conclusions

In summary, we have synthesized GaN NPs at different temperatures by chemical co-precipitation method. GaN NPs exhibit high crystalline quality with hexagonal wurtzite structure. A strong BL emission was observed for all GaN NPs irrespective of nitridation temperature. The defect related YL and RL bands disappear as the nitridation temperature increased to 1000°C due to enhancement in optical quality. The additional phonon mode at about 271-273 cm^{-1} of GaN NPs can be assigned to phonon frequency at K point of the Brillouin zone in wurtzite GaN which is not experimentally observed for their bulk counterparts. The calculated free-carrier concentration and mobility from Raman line shape analysis of coupled A_1(LO) phonon-plasmon mode are 1.36×10^{17} cm^{-3} and 433 cm^2/Vs respectively. The results demonstrate that homogeneous GaN NPs is a potential candidate as a source material for the synthesis of GaN single crystals and ceramic GaN pellet as a polycrystalline substrate for nitride based device applications.

Acknowledgement

K.J. thanks Department of Science and Technology (DST), Govt. of India for the financial assistances under the project No.SR/NM/NS-77/2008. The authors K.J and M.G acknowledge UGC-DAE Consortium for Scientific Research (CSR), Kalpakkam Node, Kokilamedu,TamilNadu, India for extending facility for TEM measurements. One of the authors M.G acknowledges Dr. P. Sangeetha, Department of Laser Studies, School of Physics, Madurai Kamaraj University, Madurai, India for the technical assistance on the micro-Raman measurements. One of the authors M.G acknowledges the award of UGC - Research fellowship in Sciences for meritorious students (RFSMS), UGC, Govt. of India.

Notes and references

[a] *Centre for Nanoscience and Nanotechnology, School of Physics, Bharathidasan University, Tiruchirappalli – 620 024, TamilNadu, India.*

[b] *Department of Laser studies, School of Physics, Madurai Kamaraj University, Madurai – 625 021, TamilNadu, India.*

[c] *UGC-DAE Consortium for Scientific Research (CSR), Kalpakkam Node, Kokilamedu – 603 104,TamilNadu, India.*
**Corresponding author E-mail – kjeganathan@yahoo.com*

1 G.Timp, Editor, *Nanotechnology*, AIP, New York, 1999.
2 J.R.Heath, Editor, *Nanoscale Materials*, special issue of *Acc. Chem. Res.*1999, 32, 5.
3 F.A.Ponce and D.P.Bour, *Nature*, 1997, 386, 351.
4 S.Nakamura, *Science*, 1998, 281, 956.
5 G.Fosal, *Science*, 1996, 272, 1751.
6 S.N.Mohammad and H.Morkoc, *Prog. Quantum. Electron*. 1996, 20, 361.
7 S.Hochi, H.Okita, Y.Morino and M.Itoh, *Oki.Tech.Rev*.2007, 74, 90.
8 P.D.Ye, B.Yang, K.K.Ng, J.Bude, G.D.Wilk, S.Halder and J.C.M.Hwang, *Appl.Phys.Lett*. 2005, 86, 063501.
9 M.A.Khan, A.Bhattarai, J.N.Kuznia and D.T.Olson, *Appl.Phys.Lett*. 1993, 63, 1214.
10 S.Sakai, S.Kurai, T.Abe and Y.Noi, *Jpn.J.Appl.Phys*.1996, 35, L77.
11 S.Porowski, *J.Cryst.Growth*, 1996,166, 583.
12 Q.Bao, H.sawayama, T.Hashimoto, F.Sato, K.Hazu, Y.Kagamitani, T.Ishinabe, M.Saito, R.Kayano, D.Tomida, K.Qiao, S.F.Chichibu, C.Yokoyama and T.Ishiguro, *CrystEngComm*. 2012,14, 3351.
13 R.Ghosh and D.Basak, *J.Appl.Phys*. 2005,98, 086104.
14 M.Nyk, R.Kudrawiec, W.Strek and J.Misiewicz, *Opt.Mater*. 2006, 28. 767.
15 R.Kudrawiec, M.Nyk, M.Syperek, A.Podhorodecki, J.Misiewicz and W.Strek, *Appl.Phys.Lett*. 2006, 88, 181916.
16 M.Nyk, R.Kudrawiec, J.Misiewicz, R.Paszkiewicz, R.Korbutowicz, J.Kozlowski, J.Serafinczuk and W.Strek, *J.Cryst.Growth,* 2005, 277, 149.
17 L.Yu, Y.Lv, X.Zhang,Y.Zhao, Y.Zhang, H.Huang and Y.Feng, *CrystEngComm*. 2010, 12, 2037.
18 S.Manna, V.D.Ashok and S.K.De, *ACS Appl.Mater.Interfaces*. 2010, 2, 3539.
19 M.Gopalakrishnan, V.Purushothaman, P.SundaraVenkatesh, V.Ramakrishnan and K.Jeganathan, *Mater.Res.Bull*. 2012, 47, 3323.
20 Z.Huizhao and X.Shoublin, *Mat. Lett*. 2008, 62, 23.
21 H.Zhuang, S.Zhang, C.Xue, B.Li, J.Shen and D.Wang, *Microelect.J*. 2008, 39, 807.
22 L.X.Qin, C.S.Xue, H.Z.Zhuang, Z.Z.Yang, H.Li, J.H.Chen and Y.Wang, *Appl. Phys. A*. 2008, 91, 675.
23 A.C.Tas, P.J.Majewski and F.Aldinger, *J.Am.Ceram.Soc.,* 2002, 85, 1421.
24 G.Li, C.Peng, C.Li, P.Yang, Z.Hou, Y.Fan, Z.Cheng and J.Lin, *Inorg.Chem*. 2010, 49, 1449.
25 Y.Zhao, R.L.Frost, J.Yang and W.N.Martens, *J.Phys.Chem.C*, 2008, 112, 3568.
26 P. Scherrer, Nachr. Ges. Wiss. Gottingen, 1918, 26, 98.
27 M.A.Reshchikov and H.Morkoc, *J.Appl.Phys*.2005, 97, 061301.
28 W.Hayes and R.Laudon, *Scattering of light by crystals*, Wiley, New York, 1978.
29 Yu. Davydov, Yu. E. Kitaev, I. N. Goncharuk, A. N. Smirnov, J. Graul, O. Semchinova, D. Uffmann, M. B. Smirnov, A. P. Mirgorodsky, R. A. Evarestov, Phys. Rev. B .1998, 58,12899.
30 C.C.Chen, C.C.Yeh, C.H.Chen, M.Y.Yu, H.L.Liu, J.J.Wu, K.H.Chen, L.C.Chen, J.Y.Peng and Y.F.Chen, *J.Am.Chem.Soc*. 2001, 123, 2791
31 X. H. Huang, Z. Y. Zhan, K. P. Pramoda,C. Zhang, L. X.Zheng and S. J. Chua, CrystEngComm, 2012, 14, 5163.
32 H.M.Tutuncu and G.P.Srivastava, *Phys.Rev.B*. 2000, 62, 5028.
33 C.Wetzel, W.Walukiewicz, E.E.Haller, J.Ager, I.Grzegory, S.Porowski and T.Suski, *Phys.Rev.B*. 1996, 53, 1322.
34 M.Kuball, *Surf.Interface Anal*. 2001, 31, 987.
35 P.Perlin, J.Camassel, W.Knap, T.Taliercio, J.C.Chervin, T.Suski, I.Grzegory and S.Porowski, *Appl.Phys.Lett*. 1995, 67, 2524.
36 E.Frayssinet, W.Knap, S.Krukowski, P.Perlin, P.Wisniewski, T.Suski, I.Grzegory and S.Porowski, *J.Cryst.Growth*, 2001, 230, 442.
37 T.Kozawa, T.Kachi, H.Kano, Y.Taga, M.Hashimoto, N.Koide, K.Manabe, *J.Appl.Phys*. 1994, 75, 1098.
38 M.Park, J.J.Cuomo, B.J.Rodriguez, W.C.Yang, R.J.Nemanich, O.Ambacher, *J.Appl.Phys*. 2003, 93, 9542.
39 D.Wang, C.C.Tin, J.R.Williams, M.Park, Y.S.Park, C.M.Park, T.W.Kang and W.C.Yang, *Appl.Phys.Lett*. 2005, 87, 242105.
40 K.Jeganathan, R.K.Debnath, R.Meijers, T.Stoica, R.Calarco, D.Grutzmacher and H.Luth, *J.Appl.Phys*. 2009, 105, 123707.

Table of Contents

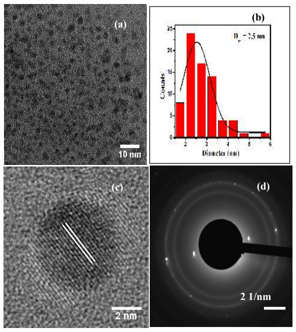

The nitridation at high temperature enhances the crystalline and optical quality of GaN nanoparticles synthesized by novel chemical co-precipitation method.